

Impact Factor:

ISRA (India) = 4.971
ISI (Dubai, UAE) = 0.829
GIF (Australia) = 0.564
JIF = 1.500

SIS (USA) = 0.912
ПИИИ (Russia) = 0.126
ESJI (KZ) = 8.997
SJIF (Morocco) = 5.667

ICV (Poland) = 6.630
PIF (India) = 1.940
IBI (India) = 4.260
OAJI (USA) = 0.350

SOI: [1.1/TAS](#) DOI: [10.15863/TAS](#)

International Scientific Journal Theoretical & Applied Science

p-ISSN: 2308-4944 (print) e-ISSN: 2409-0085 (online)

Year: 2020 Issue: 06 Volume: 86

Published: 30.06.2020 <http://T-Science.org>

QR – Issue



QR – Article



Denis Chemezov
Vladimir Industrial College
M.Sc.Eng., Corresponding Member of International Academy of Theoretical and Applied Sciences, Lecturer, Russian Federation
<https://orcid.org/0000-0002-2747-552X>
vic-science@yandex.ru

Vladimir Goremykin
Vladimir Industrial College
Master of Industrial Training, Russian Federation

Alexey Kuzin
Vladimir Industrial College
Student, Russian Federation

Alexandr Petrenko
Vladimir Industrial College
Master of Industrial Training, Russian Federation

Emil Akhmetov
Vladimir Industrial College
Student, Russian Federation

Irina Pavlakhina
Vladimir Industrial College
Lecturer, Russian Federation

Irina Medvedeva
Vladimir Industrial College
Master of Industrial Training, Russian Federation

Mikhail Ustinov
Vladimir Industrial College
Student, Russian Federation

Sergey Markov
Vladimir Industrial College
Student, Russian Federation

TO THE QUESTION OF ELECTRICAL DISCHARGE MACHINING OF THE STEEL WORKPIECE WITH THE STEEL ELECTRODE

Abstract: The impact of electric discharge on the processed surface of the steel workpiece in the conditions of electrical discharge machining with the steel cylindrical electrode was considered in the article. The electrical and thermal parameters of electrical discharge machining were calculated for the pulse duration of 0.5 s. The depth of the deformed layer of the workpiece material is presented in the three-dimensional view.

Impact Factor:

ISRA (India) = 4.971	SIS (USA) = 0.912	ICV (Poland) = 6.630
ISI (Dubai, UAE) = 0.829	PIIHQ (Russia) = 0.126	PIF (India) = 1.940
GIF (Australia) = 0.564	ESJI (KZ) = 8.997	IBI (India) = 4.260
JIF = 1.500	SJIF (Morocco) = 5.667	OAJI (USA) = 0.350

Key words: the electrode, the workpiece, electrical discharge machining, the ring, the deformed layer.

Language: English

Citation: Chemezov, D., et al. (2020). To the question of electrical discharge machining of the steel workpiece with the steel electrode. *ISJ Theoretical & Applied Science*, 06 (86), 545-550.

Soi: <http://s-o-i.org/1.1/TAS-06-86-100> **Doi:**  <https://dx.doi.org/10.15863/TAS.2020.06.86.100>

Scopus ASCC: 2209.

Introduction

Electrical discharge machining (EDM) is the progressive type of processing of various conductive materials. EDM can be carried out both with electrodes (for forming the blind profile) and with wire (for cutting the through profile). The low performance and the low-forecast tool wear are the main disadvantages of EDM. Some researches of the effective implementation of EDM are presented in the works [1-10].

Electric discharge that causes local heating of processed material passes between the surfaces of the tool and the workpiece in the process of EDM. The temperature increases intensively on the surface layers and leads to melting of the workpiece material in the short period of time. Thus, EDM includes the combination of thermomechanical, hydrodynamic,

electrical and other processes. The presentation of intensity of volumetric deformation of the workpiece material will allow to choose the rational modes for roughing or finishing EDM. Let us consider thermal deformation and changing the volume of the workpiece material during EDM with the steel electrode.

Materials and methods

The passing process of discharge current between the surfaces of the electrode (the tool) and the workpiece was modeled according to the condition of the computer experiment. The electrode was the solid cylinder. The workpiece was the solid disk. The electrode and the workpiece were made of structural steel. The models for the computer experiment are presented in the Fig. 1.

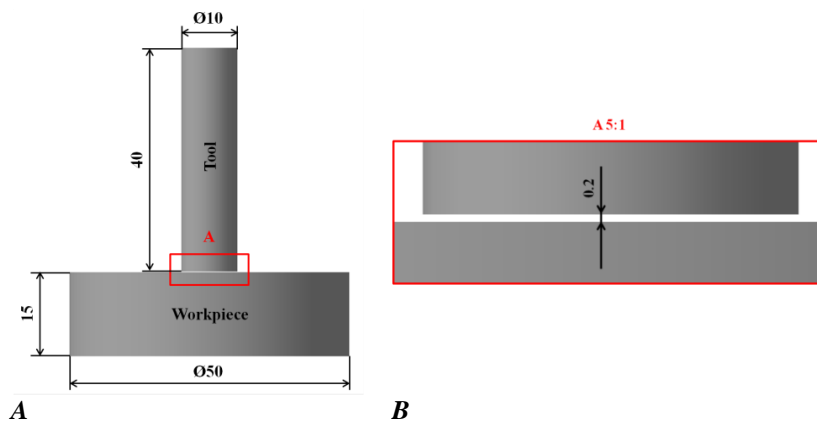


Figure 1 – The models for the experiment: A – The orientation and the models dimensions of the tool and the workpiece; B – The detail section that explains the size of the spark gap.

EDM was carried out in the gas environment. Electric discharge of 10000 mA and duration of 0.5 s occurred in the spark gap. Voltage during EDM was accepted 25000 mV.

The size of the finite element indicates the accuracy of the computer calculation. The three-

dimensional models of the tool and the workpiece after splitting into the finite elements are shown in the Fig. 2. The size of one element was accepted 1.5 mm. The mesh on the workpiece model was denser, which increased the accuracy of the simulation results in the processing zone.

Impact Factor:

ISRA (India)	= 4.971	SIS (USA)	= 0.912	ICV (Poland)	= 6.630
ISI (Dubai, UAE)	= 0.829	ПИИИ (Russia)	= 0.126	PIF (India)	= 1.940
GIF (Australia)	= 0.564	ESJI (KZ)	= 8.997	IBI (India)	= 4.260
JIF	= 1.500	SJIF (Morocco)	= 5.667	OAJI (USA)	= 0.350

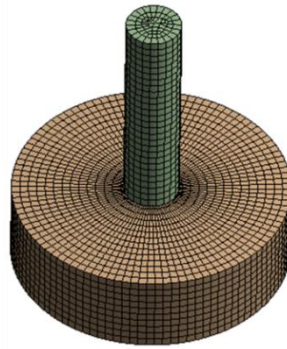


Figure 2 – The view of the models after splitting into the finite elements.

Calculation

The main part of the calculation of EDM is presented in the generated report.

***** ANSYS SOLUTION ROUTINE *****

USE A MAXIMUM OF 1 EQUILIBRIUM ITERATIONS EACH SUBSTEP

*** WARNING *** CP = 5.195

Using 1 iteration per substep may result in unconverged solutions for nonlinear analysis and the program may not indicate divergence in this case. Check your results.

DO NOT USE PREDICTOR METHOD FOR ALL DEGREES OF FREEDOM

SPECIFIED CONSTRAINT VOLT FOR PICKED NODES

REAL = _LOADVARI62 IMAG = 0.00000000

ALL SELECT FOR ITEM = NODE COMPONENT =

IN RANGE 1 TO 80428 STEP 1

80428 NODES (OF 80428 DEFINED) SELECTED BY NSEL COMMAND

SELECT COMPONENT _CM33

*GET _NODNUM FROM NODE ITEM = NUM MIN VALUE = 1483.00000

SPECIFIED NODAL LOAD AMPS FOR SELECTED NODES 1483 TO 1483 BY 1

REAL = _LOADVARI33 IMAG = 0.00000000

COUPLED SET = 1 DIRECTION = VOLT TOTAL NODES = 224

MAXIMUM COUPLED SET NUMBER = 1

ALL SELECT FOR ITEM = NODE COMPONENT =

IN RANGE 1 TO 80428 STEP 1

80428 NODES (OF 80428 DEFINED) SELECTED BY NSEL COMMAND

*** WARNING *** CP = 5.257

Element shape checking is currently inactive. Issue SHPP, ON or SHPP, WARN to reactivate, if desired.

*** WARNING *** CP = 5.413

Material number 4 (used by element 18190) should normally have at least one MP or one TB type command associated with it. Output of energy by material may not be available.

*** NOTE *** CP = 5.444

This nonlinear analysis defaults to using the full Newton-Raphson solution procedure. This can be modified using the NROPT command.

*** NOTE *** CP = 5.444

The conditions for direct assembly have been met. No .emat or .erot files will be produced.

*** NOTE *** CP = 5.444

It is highly recommended to use the solution control option by issuing the SOLCONTROL, ON command for this problem for robustness and efficiency.

*** NOTE *** CP = 6.131

It is highly recommended to use the auto contact setting option by issuing CNCHECK, AUTO command for this problem in order to achieve better convergence.

*** NOTE *** CP = 6.131

Symmetric deformable-deformable contact pair identified by real constant set 3 and contact element type 3 has been set up. The companion pair has real constant set ID 4. Both pairs should have the same behavior.

ANSYS will keep the current pair and deactivate its companion pair, resulting in asymmetric contact.

Electrostatic contact is activated.

Impact Factor:	SISRA (India) = 4.971	SIS (USA) = 0.912	ICV (Poland) = 6.630
	ISI (Dubai, UAE) = 0.829	PIIHQ (Russia) = 0.126	PIF (India) = 1.940
	GIF (Australia) = 0.564	ESJI (KZ) = 8.997	IBI (India) = 4.260
	JIF = 1.500	SJIF (Morocco) = 5.667	OAJI (USA) = 0.350

Contact detection at: Gauss integration point
Average contact surface length 1176.9
Average contact pair depth 1481.5
Default pinball region factor PINB 0.25000
The resulting pinball region 370.37
Initial penetration/gap is excluded.
Bonded contact (always) is defined.
Electric contact capacitance coef. ECC
0.65574E+12

*** NOTE *** CP = 6.131
Min. initial gap 200 was detected between
contact element 18261 and target element 18764.
The gap is closed due to initial settings.

*** WARNING *** CP = 6.131
The geometric gap/penetration may be too large.
Increase pinball radius if it is a true geometric
gap/penetration. Decrease pinball if it is a false one.

*** NOTE *** CP = 6.131
Symmetric deformable-deformable contact pair
identified by real constant set 4 and contact element
type 3 has been set up. The companion pair has real
constant set ID 3. Both pairs should have the same
behavior.

ANSYS will deactivate the current pair and keep
its companion pair, resulting in asymmetric contact.
Electrostatic contact is activated.
Contact detection at: Gauss integration point
Average contact surface length 747.17
Average contact pair depth 1500.0
Default pinball region factor PINB 0.25000
The resulting pinball region 375.01
Initial penetration/gap is excluded.
Bonded contact (always) is defined.
Electric contact capacitance coef. ECC
0.65574E+12

*** NOTE *** CP = 6.131
Min. initial gap 200 was detected between
contact element 18328 and target element 18248.
The gap is closed due to initial settings.

**SUMMARY FOR CONTACT PAIR
IDENTIFIED BY REAL CONSTANT SET 3**
Max. penetration of -7.275957614E-12 has been
detected between contact element 18276 and target
element 18733.

Max. geometrical gap of 200 has been detected
between contact element 18258 and target element
18681.

*** WARNING *** CP = 9.173
Contacting area 78538884.
Max. pinball distance 370.370007.
One of the contact searching regions contains at
least 22 target elements.

**SUMMARY FOR CONTACT PAIR
IDENTIFIED BY REAL CONSTANT SET 4**

*** NOTE *** CP = 9.173
Contact pair is inactive.

Range of element maximum matrix coefficients
in global coordinates
Maximum = 2.943955282E+17 at element
18311.

Minimum = 7.605535165E+15 at element 513.

***** ELEMENT MATRIX FORMULATION
TIMES**

TYPE NUMBER ENAME TOTAL CP AVE CP

1 1809 SOLID231 0.468 0.000259
2 16380 SOLID231 3.822 0.000233
3 413 CONTA174 0.094 0.000227
4 413 TARGE170 0.031 0.000076

Time at end of element matrix formulation CP =
9.2040596.

CURRENT CONVERGENCE VALUE =
0.1702E+20 CRITERION = 0.1702E+17

SPARSE MATRIX DIRECT SOLVER.

Number of equations = 75192, Maximum
wavefront = 551

*** NOTE *** CP = 13.806

Sparse solver maximum pivot =
5.855352997E+17 at node 1483 VOLT.

Sparse solver minimum pivot =
4.283506717E+15 at node 25678 VOLT.

Sparse solver minimum pivot in absolute value =
4.283506717E+15 at node 25678 VOLT.

***** ELEMENT RESULT CALCULATION
TIMES**

TYPE NUMBER ENAME TOTAL CP AVE CP

1 1809 SOLID231 0.312 0.000172
2 16380 SOLID231 2.480 0.000151
3 413 CONTA174 0.062 0.000151
4 413 TARGE170 0.031 0.000076

FINISH SOLUTION PROCESSING

Results and discussion

The simulation results are presented by the color
contours of the total electric field intensity, the total
current density, Joule heat and the volume on the
workpiece model (the Fig. 3). The total electric field
intensity and the total current density have the same
distribution in the volume of the workpiece model. In
the central part of the processed area of the workpiece,
intensity of these electrical parameters is less than in

Impact Factor:

ISRA (India) = 4.971	SIS (USA) = 0.912	ICV (Poland) = 6.630
ISI (Dubai, UAE) = 0.829	ПИИИ (Russia) = 0.126	PIF (India) = 1.940
GIF (Australia) = 0.564	ESJI (KZ) = 8.997	IBI (India) = 4.260
JIF = 1.500	SJIF (Morocco) = 5.667	OAJI (USA) = 0.350

the peripheral part. Maximum intensity is expressed by the contour ring.

During EDM, the heat source is partly surface in nature, partly formed by Joule heat released inside of the workpiece. Joule heat is defined as the product of the electric field intensity and the current density. Significant heat generation will occur on the periphery of the processed surface. Heat is released unevenly in the area of the contour ring.

The depth of the deformed layer of the workpiece is presented in the Fig. 3, C. The deformed

volume of the workpiece material has the sphere shape. The maximum diameter of the deformed workpiece material equal to $1.5d$ of the electrode, the maximum depth equal to $0.4d$ of the electrode (d is the electrode diameter, mm).

The workpiece volume increases in the direction from the center to the periphery at destruction of the surface layers of material. The volume increases up to 8 times. At the same time, the volume practically does not change in the most deformed material of the workpiece.

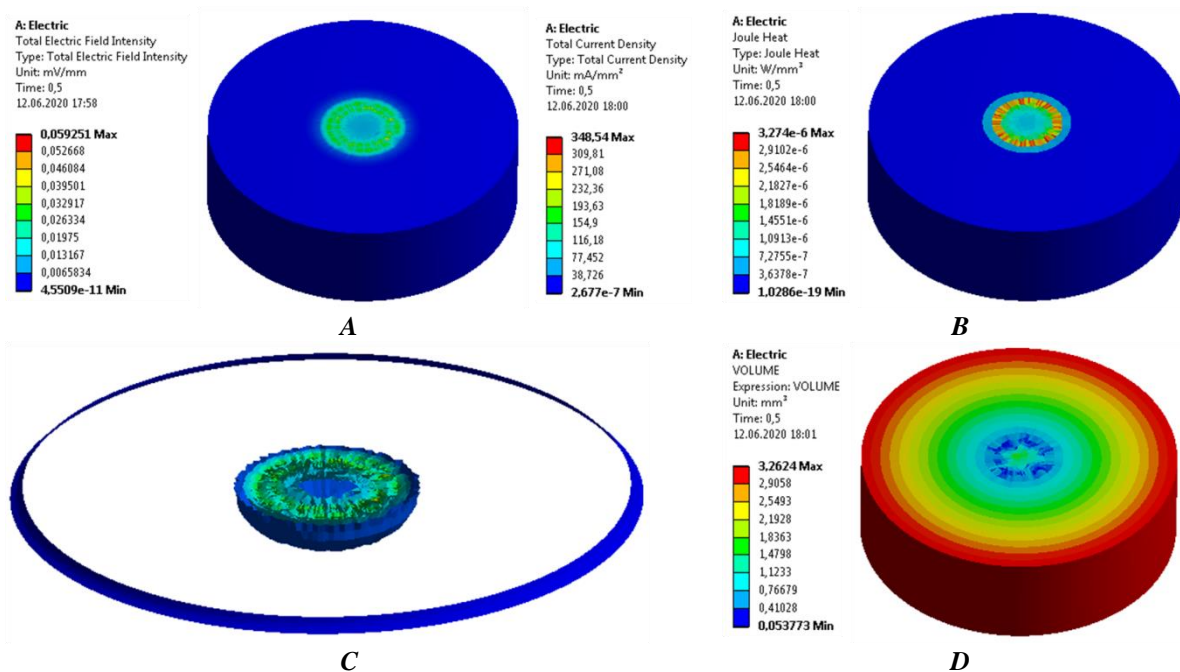


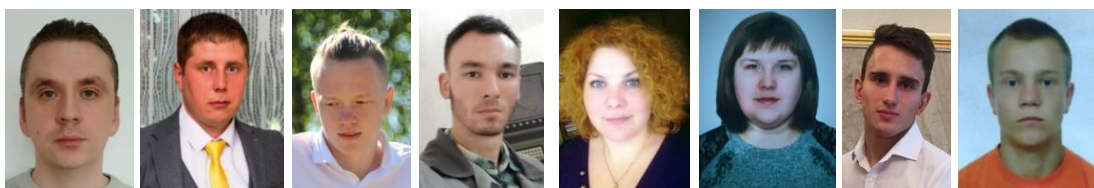
Figure 3 – The simulation results: A – The total electric field intensity and the total current density; B – Joule heat; C – The depth of the deformed layer of the workpiece; D – The volume.

Conclusion

EDM with the steel cylindrical electrode is accompanied by the formation of the peak heat ring, which is located on the periphery of the deformation

area of the steel workpiece. The depth of deformation (destruction) of material increases from the periphery to the center of the processed surface layer of the workpiece.

Authors



Denis Chemezov Vladimir Goremykin Alexey Kuzin Alexandr Petrenko Irina Pavlkhina Irina Medvedeva Mikhail Ustinov Sergey Markov

Impact Factor:

ISRA (India)	= 4.971	SIS (USA)	= 0.912	ICV (Poland)	= 6.630
ISI (Dubai, UAE)	= 0.829	PIIHQ (Russia)	= 0.126	PIF (India)	= 1.940
GIF (Australia)	= 0.564	ESJI (KZ)	= 8.997	IBI (India)	= 4.260
JIF	= 1.500	SJIF (Morocco)	= 5.667	OAJI (USA)	= 0.350

References:

1. Orlov, Yu., et al. (2019). Influence of processing modes on wear resistance of copper and graphite electrodes. *International Journal of Innovation Engineering and Science Research*, volume 3, issue 2, 1-13.
2. Pawade, M. M., & Banwait, S. S. (2013). A Brief Review of Die Sinking Electrical Discharging Machining Process towards Automation. *American Journal of Mechanical Engineering*, 1(2), 43-49.
3. Wong, Y. S., Lim, L. C., & Lee, L. C. (1995). Effects of Flushing on Electro-Discharge Machined Surfaces. *Journal of Materials Processing Technology*, 48, 299-305.
4. McGeough, J. A. (1988). Electro discharge machining in *Advanced Methods of Machining*. Chapman & Hall, London, pp. 130.
5. Kiyak, M., & Cakir, O. (2007). Examination of machining parameters on surface roughness in EDM of tool steel. *Journal of Materials Processing Technology*, 191, 141-144.
6. Ramarao, P. V., & Faruqi, M. A. (1982). Characteristics of the surfaces obtained in electro-discharge machining. *Precision Engineering*, 4/2, 111-113.
7. Lee, H. T. (1996). Influence of EDM process parameters on surface defects and roughness. *Chin. J. Mater. Sci.*, 28/4, 270-278.
8. Halkaci, H. S., & Erden, A. (2002). Experimental investigation of surface roughness in electric discharge machining. *6th Biennial Conference (ESDA 2002), Turkey*, 1-6.
9. Cogun, C., Kocabas, B., & Ozgedik, A. (2004). Experimental and theoretical investigation of workpiece surface roughness profile in EDM. *J. Fac. Engg. Arch.*, 19, 97-106.
10. Chemezov, D., et al. (2019). Stability analysis of electrical discharge machining with brass wire. *ISJ Theoretical & Applied Science*, 11 (79), 101-104.